Macroscopic Evidence of the Effect of Interfacial Slippage on Adhesion

Bi-min Zhang Newby, Manoj K. Chaudhury,* Hugh R. Brown

The adhesion strengths of a viscoelastic adhesive were measured on various substrates that were prepared by grafting silanes bearing organic functional groups to silicon wafers. Conventional theories predict that adhesion should be proportional to the surface free energy of the substrate; but adhesion on a fluorocarbon surface was significantly greater than on some of the hydrocarbon surfaces, although the fluorocarbon surface has the lowest surface free energy. This result could be explained by invoking a model of adhesion based on the slippage of the adhesive at the interface.

It is not well understood why viscoelastic adhesives, such as transparent adhesive tapes, stick to some surfaces more strongly than to others. According to conventional theories (*1, 2*) of adhesion, the energy supplied to separate an interface is largely dissipated as heat; only a small fraction of the energy is used to overcome intermolecular forces. Adhesion strength is directly proportional to the viscoelastic energy dissipation, the magnitude of which is controlled by interfacial processes. Current theories (*1, 2*) consider peeling to be the principal mode of separation of the adhesive from the substrate; thus, the adhesion strength is proportional to the surface free energy. However, our findings indicate that the adhesion of a viscoelastic adhesive is controlled not so much by the thermodynamic work of adhesion but by interfacial slippage.

We observed that the peel adhesion of a transparent tape on a fluorocarbon surface is considerably greater than that on a hydrocarbon surface, even though the surface free energy of fluorocarbon is lower than that of hydrocarbon. Furthermore, we observed that the meniscus instability patterns differ on these surfaces: the patterns are smooth on the surfaces that exhibit low peel adhesion, but elongated and irregular on the surfaces exhibiting high peel adhesion. These observations indicate that the adhesive experiences a shear resistance during the peeling process and that both the meniscus instability and the peel strength of the adhesive are influenced by the adhesive's ability to slip over the substrate.

The interfacial factors that govern adhesion of viscoelastic adhesives were examined with three types of organic surfaces. These surfaces were prepared by grafting silanes having organic functional groups onto polished silicon wafers (*3*). The first surface (FC) was prepared by formation of a self-assembled monolayer (SAM) of fluoroalkylsiloxane [$CF_3(CF_2)_7(CH_2)_2SiO_{3/2}$] onto silicon. Another surface (HC) was a SAM of alkylsiloxane [$CH_3(CH_2)_nSiO_{3/2}$, $9 \leq n \leq 15$]. The third surface (PDMS) was prepared by grafting a long chain siloxane polymer, polydimethylsiloxane [$CH_3CH_2CH_2CH_2(OSi(CH_3)_2)_n(CH_3)_2SiO_{1/2}$] onto silicon. The surface free energies (*4*) (γ_s) of these surfaces determined by the contact angle are of the following order: γ_{FC} (10 mJ/m^2) $<$ γ_{HC} (20 mJ/m^2) $\lesssim$ γ_{PDMS} (22 mJ/m^2). Values for the work of adhesion of the dispersive surfaces follow a geometric mean of their cohesive energies (*4*). Because all the surfaces (PDMS, HC, and FC) interact with the adhesive by means of dispersive interactions, their work of adhesion values [PDMS (57 to 59 mJ/m^2) $\gtrsim$ HC (55 to 56 mJ/m^2) $>$ FC (40 to 46 mJ/m^2)] follow the same sequence as their surface free energies, which has also been confirmed by direct measurements of work of adhesion with contact mechanics methods (*5*). On the basis of the trend of the surface free energies, the peel adhesion should be highest on the PDMS surface and lowest on the FC surface. However, our results show that the contrary is true.

Standard transparent tapes (*6*) were peeled from the various substrates by using a string, which ran over a pulley, that had known weights hanging from its free end. The position of the pulley was adjusted to obtain a peel angle of 40°. The experimental setup also contained video microscopic capability that allowed examination of the peeling fronts as a function of the substrate conditions. The adhesion results (summarized in Fig. 1) show that the peel velocity increases as the peel force increases for a given substrate. At a particular velocity, the peel force values vary as FC > HC > PDMS.

If the above discrepancy between the experimentally observed trend in peel adhesion and that expected from the γ_s values were to be explained by using the classic model of peel adhesion, where fracture toughness increases with work of adhesion, an unrealistic amount of surface reconstruction needs to be postulated. For example, it would require that the surface free energy of the FC surface increase to an effective value of 500 mJ/m^2—a value 50 times that of its true value. The discrepancy however may be explained by invoking a model that allows interfacial slippage. When a viscoelastic adhesive is peeled from a solid substrate, it simultaneously undergoes an extensional deformation and shrinkage at the base area of contact. If the substrate allows the adhesive to slip, the viscous work needed to carry out a rolling motion of the adhesive is lowered at the crack tip, and thus the adhesion strength is reduced.

The slippage of viscoelastic polymers on rigid solids under shear stress is known in other fields of polymer science (*7*). Migler *et al.* (*7*) measured slip velocities of a high molecular weight polymer (PDMS) on several surfaces and found direct evidence of strong slippage on a hydrocarbon monolayer. The shear response of fluids confined between rigid walls is also thought to be related to the slippage along the interfaces (*8*). In these studies, FC liquids exhibit a higher shear stress at the interface than their HC analogs. Higher friction of FC surfaces was also observed with Langmuir-Blodgett films and SAMs (*9, 10*). These observations and the studies of Brown (*11*) point out that the surfaces of greater local mobility have lower friction than the rigid ones. On the basis of this scenario, the adhesive is likely to slip most on the flexible PDMS surface and least on the FC surface. The general trend of the peel adhesion values is consistent with this phenomenological description of interfacial slippage.

To examine further the possible effect of surface mobility on peel adhesion, we used SAMs of hexadecylsilane of two different phase states. The surface with a partially

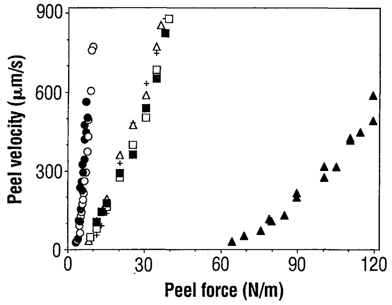

Fig. 1. The peel adhesion results of a viscoelastic adhesive on three types of surfaces at a peel angle of 40°. Within a certain class of organic film, the adhesion does not depend significantly on film thickness. PDMS: 50 Å thick (○), 100 Å thick (●); hydrocarbons: C_{10} (△), C_{11} (+), C_{14} (□), and C_{16} (■); fluorocarbon (▲).

B.-m. Zhang Newby and M. K. Chaudhury, Department of Chemical Engineering, Lehigh University, Bethlehem, PA 18015, USA.
H. R. Brown, International Business Machines, Almaden Research Center, San Jose, CA 95120, USA.

*To whom correspondence should be addressed.

covered hexadecylsiloxane [$CH_3(CH_2)_{15}SiO_{3/2}$] monolayer exhibits a liquidlike state, whereas the surface with a completely covered $CH_3(CH_2)_{15}SiO_{3/2}$ monolayer exhibits a crystalline state (*12*). Because the chains in a liquidlike monolayer are more mobile than those in a crystalline state, the liquidlike monolayer should allow more slippage than the crystalline surface and therefore yield lower adhesion, as we observed (Fig. 2).

In the language of fracture mechanics, the peel test is a combination of opening and shear modes, characterized by their respective stress intensity factors K_I and K_{II}. Thouless and Jensen (*13*) suggested that the phase angle [$\psi = \tan^{-1}(K_{II}/K_I)$] is $-38°$ under most circumstances. A negative phase angle tends to drive the crack into the upper layer, in the present case, the strip being peeled. In our opinion, the more important source of shear at the crack tip comes from the huge elastic modulus difference between the substrate and the adhesive. The size of the phase angle caused by this modulus mismatch is, as far as we know, unsolved, although Hutchinson and Suo (*14*) reported a phase angle of up to $+15°$ for much smaller mismatches. The shape of the crack tip (Fig. 3) in our studies makes it clear that the phase angle is positive, an effect that must come from the modulus mismatches, not from global peel geometry, which is corroborated by the fact that the adhesion values at a high peel angle (180°) follow a trend similar to that of a much lower peel angle (40°).

Adhesive failure occurred by a fingering process that left webs of material between the fingers that became highly stretched (Fig. 3, A to C). This phenomenon has been described by Fields and Ashby (*15*) and Urahama (*16*). Examination of the tips of the fingers showed that the distance by which the finger tip tunnels beyond the detachment point varies with the substrate. It seems likely that the contact angle between the adhesive and the substrate (θ in Fig. 3D) varies in a similar way.

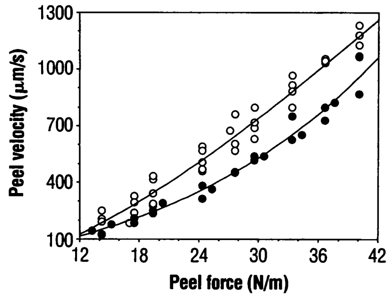

Fig. 2. The peel adhesion values on hexadecylsiloxane monolayers as a function of their phase states. The liquidlike monolayer (○) with a 65% surface coverage has lower adhesion than a completely crystalline monolayer (●).

Modeling the detachment of a pressure-sensitive adhesive is problematic because the material is essentially viscoelastic. Zosel (*17*) and Chang (*18*) showed that optimum adhesion is obtained when the storage and loss moduli of the material are both ~10 to 100 kPa at frequencies of ~1 Hz. We propose a simple model of the energy dissipation close to the crack tip in which the geometry is controlled by the elastic properties of the material, but the dissipation is estimated with the assumption that the material is viscous. If the adhesive is considered to be elastic with an effective shear modulus G, the angle θ can be related to G and the maximum shear stress (σ_s) at the interface. We assume that the interface shows static friction; there is no slip at a shear stress below σ_s but unlimited slip can occur at σ_s. The actual detachment process must occur in two ways. The situation is similar to the dewetting of a liquid. If there is no slip at the interface, the detachment must be entirely by the highly dissipative rolling motion in a wedge discussed by Dussan and Davis (*19*) and de Gennes (*20*). If there is interface slip, there can also be partial detachment by slip, as the slip process permits extension of the adhesive normal to the interface. Both of these processes are modified from the situation in a simple liquid by the finite deformation capability of the adhesive. The dissipation in the wedge in either a wetting or dewetting process increases as the angle θ decreases. Hence, as σ_s is decreased, θ increases and the viscous dissipation close to the interface decreases.

The relation between the wedge angle θ and the shear strain can be found by assuming a very crude model for the wedge deformation in which the undeformed material is considered in two regions: one in front and the other behind the crack tip. The regions experience large shear strains of equal magnitude but of opposite sign. The region behind the crack tip also rotates by $\pi - \theta$.

$$\varepsilon_{xy} = \tan[(\pi - \theta)/2] \tag{1}$$

$$\tan\theta = \frac{2G}{\sigma_s\left[1 - \left(\frac{G}{\sigma_s}\right)^2\right]} \tag{2}$$

The dissipation of viscous energy, $\mathring{Q}$, in a wedge is given by (*20*)

$$\mathring{Q} = \frac{3\eta u^2}{\tan\theta}\ln\left|\frac{x_{\max}}{x_{\min}}\right| \tag{3}$$

where u is the difference between the macroscopic velocity and the slip velocity at the interface, η is the fluid viscosity, and $x_{\max}$ and $x_{\min}$ are the maximum and minimum widths of the wedge. For fluids, $x_{\min}$ is often a molecular size, but in the adhesive case it would seem most likely that $x_{\min}$ is controlled by strain hardening that must occur in the stress concentration at the tip of the wedge. The important feature is that it should be a fixed constant. In that $x_{\max}$ is the distance between the tip of the finger and the substrate, the logarithmic term can be considered approximately equal to a constant, α. It should be noted that for non-Newtonian fluids, η will be a strain rate–dependent function.

If σ_s/G is large, the energy dissipated per unit area of new crack, G_o, can be written

$$G_o = \frac{\mathring{Q}}{u} = \frac{3\eta u\alpha\sigma_s}{2G} \tag{4}$$

demonstrating that dissipation at the local crack tip increases with the resistance to interfacial slip. In Eq. 4, G_o appears as a product of the viscous dissipation and the interfacial shear stress. It exhibits a parallelism to the theory of Gent and Schultz (*1*), except that in our model the interfa-

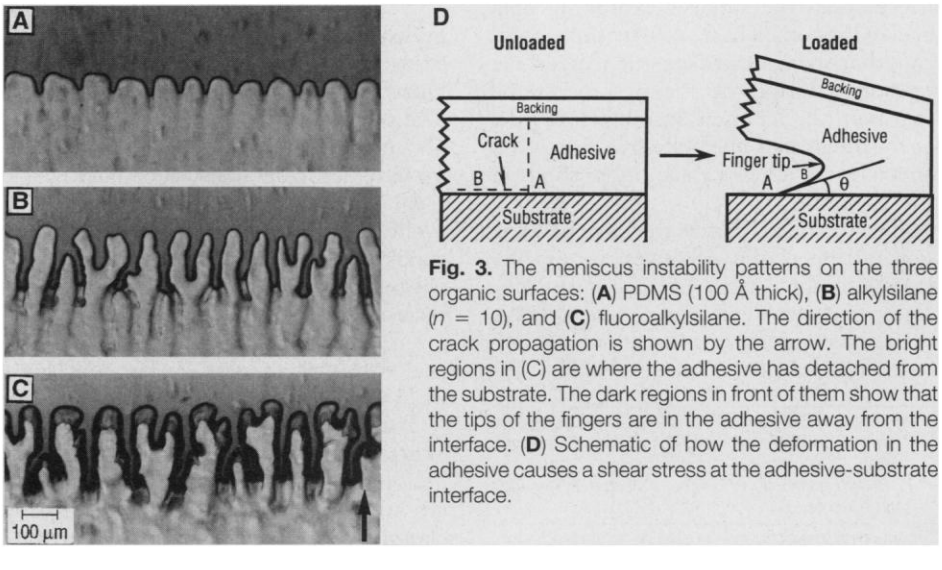

Fig. 3. The meniscus instability patterns on the three organic surfaces: (**A**) PDMS (100 Å thick), (**B**) alkylsilane (n = 10), and (**C**) fluoroalkylsilane. The direction of the crack propagation is shown by the arrow. The bright regions in (C) are where the adhesive has detached from the substrate. The dark regions in front of them show that the tips of the fingers are in the adhesive away from the interface. (**D**) Schematic of how the deformation in the adhesive causes a shear stress at the adhesive-substrate interface.

cial shear stress provides the necessary boundary condition for viscoelastic deformation rather than the thermodynamic work of adhesion.

According to this simple picture of energy dissipation at the crack tip, the shear stress at the FC surface turns out to be about four to six times that of the HC surface (see Fig. 1). Interestingly, similar ratios of shear stresses were observed in the direct measurement (*9*) of the interfacial friction of several materials against FC and HC monolayers.

The ratio η/G in Eq. 4 is the slow response time (*21*) of the adhesive, which is ~2 to 3 s. The value of α is ~10 to 15 (*22*). If we use the shear stresses (1 to 100 kPa) of rubber sliders (*9*, *10*, *23*) against rigid walls as the approximate values of σ_s, G_o is estimated to be in the range of 4 to 400 N/m for u = 100 μm/s. The experimentally observed peel forces fall well within this range. This kind of quantitative comparison, however, should not be taken too far, because the equations for the viscous energy dissipation (Eqs. 3 and 4) are strictly valid for low contact angles (or high σ_s), that is, Fig. 3C. Furthermore, our model does not include extensional deformation of the adhesive. Nevertheless, this simple calculation shows that the local viscous energy dissipation at the crack tip can be quite substantial, and its magnitude decreases as the interfacial slippage increases.

REFERENCES AND NOTES

1. A. N. Gent and J. Schultz, *J. Adhes.* **3**, 281 (1972).
2. E. H. Andrews and A. J. Kinloch, *Proc. R. Soc. London Ser. A* **332**, 385 (1973); R. J. Good and R. K. Gupta, *J. Adhes.* **26**, 13 (1988).
3. Both the hydrocarbon and fluorocarbon monolayers were prepared by reacting the silicon wafer to the vapor of alkyltrichlorosilanes [$CH_3(CH_2)nSiCl_3$, $9 \leq n \leq 15$] and fluoroalkyltrichlorosilane [$CF_3(CF_2)_7(CH_2)_2SiCl_3$] according to the methods described by M. K. Chaudhury and G. M. Whitesides [*Langmuir* **7**, 1013 (1991)]. PDMS [$CH_3CH_2CH_2CH_2(OSi(CH_3)_2)_n(CH_3)_2SiH$] was chemically grafted to the silicon wafer by reacting its Si–H groups to the surface silanols by using a platinum catalyst. Two PDMS polymers with weight-average molecular weights of 8612 and 33187 were used to yield films of thickness 50 and 100 Å, respectively.
4. The surfaces were examined with two liquids, water and hexadecane. The advancing (θ_a) and receding (θ_r) contact angles were PDMS (water: θ_a = 108°, θ_r = 106°; hexadecane: θ_a = 42°, θ_r = 32°), HC (water: θ_a = 114° to 117°, θ_r = 108° to 112°; hexadecane: θ_a = 44° to 46°, θ_r = 43° to 45°), and FC (water: θ_a = 118°, θ_r = 106°; hexadecane: θ_a = 81°, θ_r = 75°). The surface free energy was estimated from the average of the advancing and receding contact angles of hexadecane and by using the equation of Good, Girifalco, and Fowkes [L. A. Girifalco and R. J. Good, *J. Phys. Chem.* **61**, 904 (1957); F. M. Fowkes, *Ind. Eng. Chem.* **56**, 40 (1964)].
5. K. L. Johnson, K. Kendall, A. D. Roberts, *Proc. R. Soc. London Ser. A* **324**, 301 (1971).
6. A standard 3M scotch tape (catalog number of 34-7032-3525-8) was used as the adhesive material.
7. K. B. Migler, H. Hervet, L. Leger, *Phys. Rev. Lett.* **70**, 287 (1993); K. B. Migler, G. Massey, H. Hervet, L. Leger, *J. Phys. Condens. Matter* **6**, A301 (1994), and references therein.
8. G. Reiter, A. L. Demirel, J. Peanasky, L. L. Cai, S. Granick, *J. Chem. Phys.* **101**, 2606 (1994); G. Reiter, A. L. Demirel, S. Granick, *Science* **263**, 1741 (1994).
9. B. J. Briscoe and D. C. B. Evans, *Proc. R. Soc. London Ser. A* **380**, 389 (1982); V. DePalma and N. Tillman, *Langmuir* **5**, 868 (1989); R. M. Overney *et al.*, *Nature* **359**, 133 (1992).
10. M. K. Chaudhury and M. J. Owen, *Langmuir* **9**, 29 (1993).
11. H. R. Brown, *Science* **263**, 1411 (1994).
12. The phase states of the monolayer were varied by controlling the concentration of the silane in the vapor phase. Details can be found in M. K. Chaudhury and M. J. Owen, *J. Phys. Chem.* **97**, 5722 (1993).
13. M. D. Thouless and H. M. Jensen, *J. Adhes.* **38**, 185 (1992).
14. J. W. Hutchinson and Z. Suo, *Adv. Appl. Mech.* **29**, 63 (1992).
15. R. J. Fields and M. F. Ashby, *Philos. Mag.* **33**, 33 (1976).
16. Y. Urahama, *J. Adhes.* **31**, 47 (1989).
17. A. Zosel, *ibid.* **34**, 201 (1991).
18. E. P. Chang, *ibid.*, p. 189.
19. V. E. Dussan and S. Davis, *J. Fluid Mech.* **65**, 71 (1974).
20. P. G. de Gennes, *Rev. Mod. Phys.* **57**, 828 (1985).
21. The response time of the adhesive was estimated by studying the free relaxation of the Schallamach ridges [A. Schallamach, *Proc. R. Soc. London Ser. B* **66**, 386 (1953)], which were formed by sliding a rubber slider over the adhesive.
22. T. Ondarcuhu and M. Veyssie, *J. Phys. Paris* **II1**, 75 (1991).
23. M. Barquins, *Mater. Sci. Eng.* **73**, 45 (1985).
24. M.K.C. thanks A. N. Gent for valuable discussions. We thank Dow Corning Corporation and IBM for supporting this work.

26 April 1995; accepted 27 June 1995

Direct Evaluation of Electronic Coupling Mediated by Hydrogen Bonds: Implications for Biological Electron Transfer

Peter J. F. de Rege, Scott A. Williams,* Michael J. Therien†

Three supramolecular bischromophoric systems featuring zinc(II) and iron(III) porphyrins have been synthesized to evaluate the relative magnitudes of electronic coupling provided by hydrogen, σ, and π bonds. Laser flash excitation generates the highly reducing singlet excited state of the (porphinato)zinc chromophore that can subsequently be electron transfer quenched by the (porphinato)iron(III) chloride moiety. Measurement of the photoinduced electron transfer rate constants enables a direct comparison of how well these three types of chemical interactions facilitate electron tunneling. In contrast to generally accepted theory, electronic coupling modulated by a hydrogen-bond interface is greater than that provided by an analogous interface composed entirely of carbon-carbon σ bonds. These results bear considerably on the analysis of through-protein electron transfer rate data as well as on the power of theory to predict the path traversed by the tunneling electron in a biological matrix; moreover, they underscore the cardinal role played by hydrogen bonds in biological electron transfer processes.

Ascertaining how the structural complexities of proteins and membranes impact long-range donor-acceptor (D-A) interactions has long been a primary focus for both theory and experiment in the field of biological electron transfer (ET) (*1*). Beratan and Onuchic recognized that the anisotropic nature of the protein medium likely gave rise to significant variations in how well distinct regimes of polypeptide secondary and tertiary structure effected the propagation of a tunneling electron wave function (*2*). These theoretical studies led to the development of algorithms to estimate the magnitude of electronic coupling between redox sites in a biological matrix as well as predict the pathway traversed by the tunneling electron (*3*). This "pathway model" for biological electron transport relies on the premise that covalent bonds, hydrogen (H) bonds, and van der Waals contacts between atoms all modulate electronic coupling differently; hence, the extent of the decay of the tunneling electron wave function (that is, the electronic coupling between D and A) depends critically on the number of each of these chemical interactions that defines a physical ET pathway connecting D to A.

Since the first through-protein ET experiments demonstrating that the pathway model correctly predicted a specific H-bonding interaction to be critical in establishing long-range D-A electronic coupling (*4*), this method of theoretical analysis has provided (i) insight into the nature of the groups of atoms that comprise the important ET pathways in biological systems and (ii) a basis for rationalizing the magnitude of experimental ET rate constants for redox reactions involving the cytochromes (*5*), azurin (*6*), catalase (*7*), protein-protein complexes (*8*), the photosynthetic reaction center (*9*), as well as peptide

---

Department of Chemistry, University of Pennsylvania, Philadelphia, PA 19104–6323, USA.

*Present address: Department of Imaging and Photographic Technology, Rochester Institute of Technology, Rochester, NY 14623, USA.

†To whom correspondence should be addressed.